Determination of complex absorbing potentials from the electron self-energy

Thomas M. Henderson, Giorgos Fagas*, Eoin Hyde, and James C. Greer

Tyndall National Institute, Lee Maltings, Prospect Row, Cork, Ireland

(Dated: February 6, 2008)

The electronic conductance of a molecule making contact to electrodes is determined by the coupling of discrete molecular states to the continuum electrode density of states. Interactions between bound states and continua can be modeled exactly by using the (energy-dependent) self-energy, or approximately by using a complex potential. We discuss the relation between the two approaches and give a prescription for using the self-energy to construct an energy-independent, non-local, complex potential. We apply our scheme to studying single-electron transmission in an atomic chain, obtaining excellent agreement with the exact result. Our approach allows us to treat electron-reservoir couplings independent of single electron energies, allowing for the definition of a one-body operator suitable for inclusion into correlated electron transport calculations.

PACS numbers: 03.65.Nk 05.60.Gg 73.63.-b

I. INTRODUCTION

Initiated by experimental advances, interest has been growing in the first-principles description of quantum transport through nanojunctions formed by a single-molecule bridge between electrodes acting as electron reservoirs (see Ref. 1 for a recent overview). Molecular electronic structure, including its response to external fields, are well-described by *ab initio* methods if many-electron methods are used. Recent studies also point to the need for a detailed quantum chemical approach to predict current-voltage characteristics for electron transport across single molecules[2,3,4,5,6]. Unfortunately, the interaction of the molecular energy states with the bulk electrode density of states makes explicit treatment of the many-electron problem intractable.

Similar coupling of bound and continuum states occurs in many diverse processes in chemistry and physics but a completely first principles description is generally difficult. For example, with conventional, basis-set-dependent methods, it is not feasible to efficiently describe both bound and continuum states simultaneously. However, it has been known for some time that a reduced description for a finite number of degrees of freedom can be formally achieved by adding to the uncoupled Hamiltonian of the selected subsystem a non-Hermitian effective interaction[7,8,9,10]. As a result of this extra term, the line spectrum of the uncoupled Hamiltonian evolves so that the sharp energy levels become resonances with broadenings and shifts that depend on the form and strength of the coupling to the continuum.

An exact non-Hermitian interaction can be obtained through the Feshbach-Fano[11,12,13] projection operator technique and is essentially the self-energy of Green's function methods[10,14,15,16,17,18]. It is not entirely clear how best to proceed in the general case but there are now standard numerical methods to extract a first-principles self-energy for bulk electrodes in the single-particle approximation[1]. For certain model systems, analytical expressions are available[19,20]. If we could use this coupling to the reservoirs, we could describe quantum transport through a nanojunction using sophisticated many-body methods on a region (e.g., an "extended" molecule including the molecule plus some part of the leads) while retaining a single particle description of the bulk electrodes. This would open up the possibility to improve on the commonly employed but controversial single-particle description of single-molecule devices[3,4,5,6]. However, application of one-electron self-energies in many-electron calculations is not straightforward, as the single particle levels coupled to reservoirs through the self-energy terms have no immediate corresponding quantities within correlated electronic theories. Hence we seek a method that is able to transmit the information contained within the self-energies, e.g., the coupling to electron-reservoirs, directly to a many-electron description.

The formally exact complex-scaling technique provides just such an alternative[9]. By applying a complex-coordinate transformation to the Hamiltonian via smooth-exterior-scaling the Schrödinger equation is transformed; the eigenvalues remain the same but the wave functions obey different boundary conditions. This yields exact resonant positions and widths. However, for the specific applications we have in mind it is operationally more convenient to use another general means that is commonly employed and only requires the addition of an energy-independent, phenomenological complex potential to the Hamiltonian[7,8].

These potentials are typically local in space and purely imaginary, with negative imaginary part; they vanish inside the subsystem region (well-described by the usual basis set), and grow rapidly away from that region. The negative imaginary walls cause asymptotic damping of resonant eigenfunctions, preventing them from extending to infinity. The wave function becomes square-integrable, obviating the need to describe free-particle states or the associated continuum. Hence, standard bound-state methods can be applied to open systems. Because these

*Corresponding author. E-mail: gfagas@tyndall.ie

potentials effectively absorb particles that would otherwise escape to infinity, they are known as complex absorbing potentials (CAPs).

Calculations may depend rather sensitively on the detailed form of the CAP[21,22,23,24,25], and one must therefore be careful in constructing and parameterizing the complex potential. Semi-classical arguments have been used to suggest a form[26,27,28], and constraints on the form are known[29]. Parameters are sometimes fit to experiment; more frequently they are numerically optimized so that the stationarity condition for the complex-value of the resonant energy is satisfied.[29] Deviations occur because in practice complex potentials not only absorb particles but also cause artificial reflections. In fact though, Riss and Meyer[30] and Moiseyev[31] pointed out that there is a relation between complex-scaling and CAPs in the limit of zero reflections which may be used to introduce exact reflection-free CAPs; the parameters in their functional form are determined by further stability conditions[31].

While the utility of the complex potential approach has been demonstrated many times[7,8], we require a technique which allows us to avoid a search over parameter space if we are to study molecules interacting with large electron reservoirs. Further, we would like to make use of the well-understood techniques for calculating the first-principles self-energy for bulk electrodes. This suggests relating the self-energy with an energy-independent complex absorbing potential. This CAP could then be used in a many-body calculation as an additional one-body potential, similar to other applications of complex absorbing potentials[32,33]. This would allow us to apply many-body methods on a region while using the self-energy transformed CAP to couple to the reservoirs.

In this paper, our purpose is to present a method to determine a CAP starting from the self-energy. As as first application of our approach we calculate the transmission spectrum of independent electrons propagating through a model electrode-molecule-electrode junction that has been previously reported from calculations using both exact methods[19,34] and a numerically optimized CAP[35]. Remarkable agreement with the exact result is found, thus substantiating a link between the exact self-energy and an energy-independent CAP.

The structure of the paper is as follows. In Sec. II, we introduce background theoretical material for the coupling of bound states to a continuum and derive our CAP from the self-energy. Section III summarizes the application of our method to single-electron transmission through a simple model for an electrode-molecule-electrode junction described in Sec. III A. The results of our calculations are presented in Sec. III B. We conclude with a summarizing section.

II. THEORY

In order to exploit the apparent relation between the self-energy and the complex absorbing potential, we assume that an energy-independent Hamiltonian with the "correct" broadened and shifted energy levels and states contains all the relevant physics from the interaction to the continuum. We must simply define these energy levels and states and then build the operator.

A. Coupled States and Broadened Energies from the Self-Energy

Suppose we have a bare Hamiltonian H_0 which describes a closed, finite system. The fact that the system is closed and finite means that H_0 will have bound states $|\chi_i\rangle$ with sharp energies ϵ_i. That is, we have

$$H_0|\chi_i\rangle = \epsilon_i|\chi_i\rangle, \tag{1a}$$
$$\langle\chi_j|H_0 = \epsilon_j\langle\chi_j|, \tag{1b}$$
$$\langle\chi_i|\chi_j\rangle = \delta_{ij}. \tag{1c}$$

If we now couple our system to a continuum (or, equivalently, give it infinite extent), the energy levels ϵ_i will become $\omega_i = \epsilon_i + \delta_i - i\lambda_i$, where δ_i is a shift in the position of the energy level and λ_i is a width, and the states described by $|\chi_i\rangle$ will change. Our goal is to obtain these new energy levels and states.

This can be achieved in a formally exact way using the self-energy Σ from Green's function theory; the proper states and energy levels can be obtained by solving the Dyson equation. That is, we solve[36]

$$[H_0 + \Sigma(\omega_i)]|\psi_i\rangle = \omega_i|\psi_i\rangle, \tag{2a}$$
$$\langle\phi_i|[H_0 + \Sigma(\omega_i)] = \omega_i\langle\phi_i|; \tag{2b}$$

the real part of ω_i gives the position of the ith resonance including the shift from ϵ_i, and the imaginary part gives the level broadening. There will almost always be more solutions of this equation than there were eigenvalues of our original bare Hamiltonian. The extra solutions correspond to states dominated by the continuum to which we have coupled, and in these states we are not particularly interested. We need some process, then, to find the states and energy levels that best correspond to the states and energy levels of the bare Hamiltonian.

To do this, we solve the related problem

$$[H_0 + \lambda\Sigma(\omega_i^\lambda)]|\psi_i^\lambda\rangle = \omega_i^\lambda|\psi_i^\lambda\rangle, \tag{3a}$$
$$\langle\phi_i^\lambda|[H_0 + \lambda\Sigma(\omega_i^\lambda)] = \omega_i^\lambda\langle\phi_i^\lambda|. \tag{3b}$$

At $\lambda = 0$, we have the original states $|\chi_i\rangle$ and energy levels ϵ_i, while at $\lambda = 1$, we have the target states and energy levels. We simply let λ go adiabatically from 0 to 1, thereby obtaining the desired states $|\psi_i\rangle$ and $\langle\phi_i|$ and energy levels ω_i.

B. Definition of the CAP Operator

In principle, we would like to build an energy-independent complex potential W such that the Hamiltonian $H_0 + W$ has the ω_i as eigenvalues, and the $\langle\phi_i|$ and $|\psi_i\rangle$ as left- and right-hand eigenvectors. Unfortunately, we cannot actually construct such a Hamiltonian. This is because if $\langle\phi_i|$ and $|\psi_j\rangle$ are eigenvectors of the same Hamiltonian, they must satisfy $\langle\phi_i|\psi_j\rangle = \delta_{ij}$. But because we obtain $\langle\phi_i|$ and $|\psi_j\rangle$ at different energies $\omega_i \neq \omega_j$, they do not obey this biorthogonality relationship. We must therefore consider constructions which yield eigenvalues that are approximately the ω_i and eigenvectors that are approximately the $\langle\phi_i|$ and $|\psi_i\rangle$ while obeying the biorthogonality constraint. If we have approximate left- and right-eigenvectors $\langle\phi_i'|$ and $|\psi_i'\rangle$ and eigenvalues ω_i', we can define

$$W = \sum_i |\psi_i'\rangle\omega_i'\langle\phi_i'| - H_0. \tag{4}$$

Then by construction, $H_0 + W$ will have the desired eigenvalues and eigenvectors so long as $\langle\phi_i'|\psi_j'\rangle = \delta_{ij}$. We consider several ways to proceed.

The simplest approach is to build $H_0 + W$ using the eigenvectors of H_0. That is, we could define

$$W_0 = \sum_i |\chi_i\rangle\omega_i\langle\chi_i| - H_0. \tag{5}$$

This assumes that getting the proper broadening and shifts is all that is really needed to capture the proper physics.

Our next step is to introduce the dual spaces to $|\psi_i\rangle$ and $\langle\phi_i|$. That is, we have vectors $\langle\bar\psi_i|$ and $|\bar\phi_i\rangle$ which satisfy $\langle\bar\psi_i|\psi_j\rangle = \delta_{ij}$ and $\langle\phi_i|\bar\phi_j\rangle = \delta_{ij}$. With these in hand, we can now build two approximations to W, namely

$$\bar W^\psi = \sum_i |\psi_i\rangle\omega_i\langle\bar\psi_i| - H_0, \tag{6a}$$

$$\bar W^\phi = \sum_i |\bar\phi_i\rangle\omega_i\langle\phi_i| - H_0. \tag{6b}$$

Both $H_0 + \bar W^\psi$ and $H_0 + \bar W^\phi$ have the correct eigenvalues; the former gives the correct right-hand eigenvectors but rotated left-hand eigenvectors, and the latter does the opposite. Provided we are able to define the dual spaces, (6a) and (6b) give different potentials. However, we expect them to yield identical results as the same physics is carried by either the left- or right- hand eigenfunctions.

Finally, we consider a further alternative. We define

$$\bar W = \frac{\bar W^\psi + \bar W^\phi}{2}, \tag{7}$$

which assumes that symmetrizing will have useful effects. In this case, however, neither the eigenvalues nor the eigenvectors will be correct.

Note that, to lowest order in $G_0\Sigma$, where G_0 is the bare Green's function (that is, $G_0 = [\epsilon_i - H_0 + i\eta]^{-1}$), the various states we use to build the sundry approximations to

W are the same, so one expects that all these energy-independent approximations to the self-energy would yield roughly similar results. Also, we have really defined the complex potential in Hilbert space, and not as some explicit real-space function. In general, W may be non-local and have both real and imaginary parts, like $\Sigma(E)$ and unlike the phenomenological complex potentials in use.

C. Matrix Formulation

It may prove helpful to put everything in matrix language briefly. We suppose we have a bare Hamiltonian matrix $\mathbf{H}_0$, which has eigenvectors $\mathbf{X}$ so that the eigenvalue problem of (1) becomes

$$\mathbf{H}_0\mathbf{X} = \mathbf{X}\boldsymbol\epsilon, \tag{8a}$$

$$\mathbf{X}^\dagger\mathbf{H}_0 = \boldsymbol\epsilon\mathbf{X}^\dagger, \tag{8b}$$

$$\mathbf{X}^\dagger\mathbf{X} = \mathbf{1}. \tag{8c}$$

Once we add the self-energy matrix $\boldsymbol\Sigma(E)$, the Dyson equation of (2) becomes

$$[\mathbf{H}_0 + \boldsymbol\Sigma(\omega_i)]\,\mathbf{U}_i = \omega_i\mathbf{U}_i, \tag{9a}$$

$$\mathbf{V}_i^\dagger\,[\mathbf{H}_0 + \boldsymbol\Sigma(\omega_i)] = \omega_i\mathbf{V}_i^\dagger. \tag{9b}$$

We build up total eigenvector matrices $\mathbf{U}$ and $\mathbf{V}^\dagger$ from the individual eigenvectors, and similarly build a total eigenvalue matrix $\boldsymbol\omega$. Note that by taking the transpose of (9b), we see that if both $\mathbf{H}_0$ and $\boldsymbol\Sigma(\omega_i)$ are symmetric matrices, then $\mathbf{V}^\star = \mathbf{U}$ so that $\mathbf{V}^\dagger = \mathbf{U}^\mathrm{T}$.

Our various approximations for the complex potential then give us

$$\mathbf{W}_0 = \mathbf{X}\boldsymbol\omega\mathbf{X}^\dagger - \mathbf{H}_0, \tag{10a}$$

$$\bar{\mathbf{W}}^\psi = \mathbf{U}\boldsymbol\omega\mathbf{U}^{-1} - \mathbf{H}_0, \tag{10b}$$

$$\bar{\mathbf{W}}^\phi = \mathbf{V}^{-\dagger}\boldsymbol\omega\mathbf{V}^\dagger - \mathbf{H}_0, \tag{10c}$$

$$\bar{\mathbf{W}} = \frac{\bar{\mathbf{W}}^\psi + \bar{\mathbf{W}}^\phi}{2}. \tag{10d}$$

If $\mathbf{V}^\dagger = \mathbf{U}^\mathrm{T}$, then $\bar{\mathbf{W}}$ is symmetric.

III. APPLICATION

In the previous section, we presented a formal derivation of an energy-independent CAP from the self-energy that couples the subspace Hamiltonian to the continuum states. In what follows, we test the various approximations for the complex potential W and examine its structure in the case of transmission of electrons through an atomic chain.

A. Model System

To simplify the calculations and to compare with previous results based on the more conventional form of CAPs,

we turn to a simple Hückel model for an atomic chain with one orbital per atomic site and nearest neighbour interactions. Physically, this is intended as a (very simplistic) treatment of an electrode-molecule-electrode system. Typical molecular junctions are made of π-conjugate carbon chains bonded by anchor groups to metal electrodes.

Our model Hamiltonian reads

$$H = H_L + H_M + H_R + V, \tag{11}$$

where $H_{L(R)}$ describes the left (right) electrode, H_M describes the molecule, and V describes the electrode-molecule coupling. Using the c_i^k $((c_i^k)^\dagger)$ operator that creates (annihilates) an electron on the ith site of region k, the various components of the Hamiltonian are

$$H_L = \sum_{i=1}^{\infty} [\varepsilon_L (c_i^L)^\dagger c_i^L - \gamma_L (c_i^L)^\dagger c_{i\pm1}^L], \tag{12a}$$

$$H_R = \sum_{i=1}^{\infty} [\varepsilon_R (c_i^R)^\dagger c_i^R - \gamma_R (c_i^L)^\dagger c_{i\pm1}^R], \tag{12b}$$

$$H_M = \sum_{i=1}^{N} [\varepsilon_M (c_i^M)^\dagger c_i^M - \gamma_M (c_i^L)^\dagger c_{i\pm1}^M], \tag{12c}$$

$$V = -[(\Gamma_L (c_1^L)^\dagger c_1^M + \Gamma_R (c_N^M)^\dagger c_1^R) + \text{h.c.}]. \tag{12d}$$

Unless stated otherwise, we take $\varepsilon_L = \varepsilon_R = \varepsilon_M = \epsilon_0$, $\gamma_L = \gamma_R = \gamma_M = \gamma$, and $\Gamma_L = \Gamma_R = \gamma/2$. The same model has been studied using the exact self-energy[19,34], and has also been investigated with a complex potential of the usual type[35].

The Hamiltonian of (12) has an infinite number of degrees of freedom due to the infinite size of the electrodes. We relate to our previous discussion in sections I and II by considering N_L (N_R) sites from the left (right) electrode and the N sites representing the molecule. The bare Hamiltonian matrix $\mathbf{H}_0$ of this subsystem is thus of dimension $N_T = N_L + N + N_R$, and is tridiagonal; the diagonal elements are all filled with ϵ_0, and the subdiagonal (and superdiagonal) elements are given by $-\gamma$, except for the elements that represent the coupling between the molecule and the electrode, which are given by $-\Gamma$.

The self-energy needed to account for the rest of the (infinite) electrodes (i.e., to describe the coupling to the continuum) can be calculated exactly for this model[19]. The expression reads

$$\Sigma(E) = \begin{cases} \gamma(\eta - i\sqrt{1-\eta^2}) & : \quad |\eta| \leq 1, \\ \gamma(\eta - \sqrt{\eta^2-1}) & : \quad \text{else,} \end{cases} \tag{13}$$

where

$$\eta = \frac{E - \epsilon_0}{2\gamma}. \tag{14}$$

Note that if we do not explicitly include any of the electrode sites, i.e., we take $N_L = 0$ or $N_R = 0$, we must scale the self-energy for that electrode by $(\Gamma/\gamma)^2$.

In any event, the total self-energy matrix $\mathbf{\Sigma}(E)$ can be written as the sum of the self-energy matrices for the left and right electrodes, respectively $\mathbf{\Sigma}_L(E)$ and $\mathbf{\Sigma}_R(E)$, which are given by

$$[\mathbf{\Sigma}_L(E)]_{ij} = \begin{cases} \Sigma(E) & : \quad i = j = 1, \\ 0 & : \quad \text{else,} \end{cases} \tag{15a}$$

$$[\mathbf{\Sigma}_R(E)]_{ij} = \begin{cases} \Sigma(E) & : \quad i = j = N_T, \\ 0 & : \quad \text{else.} \end{cases} \tag{15b}$$

B. Results

Using the self-energy of (15), one can calculate the transmission function through the molecule via

$$T(E) = \text{tr}(\mathbf{\Lambda}_L \, \mathbf{G} \, \mathbf{\Lambda}_R \, \mathbf{G}^\dagger), \tag{16}$$

where $\mathbf{G} = [E - (\mathbf{H}_0 + \mathbf{\Sigma}(E))]^{-1}$ is the Green's function matrix, and $\mathbf{\Lambda}_L$ and $\mathbf{\Lambda}_R$ are the spectral densities for the left and right electrode, respectively, defined in terms of the self-energies as

$$\mathbf{\Lambda}_{L(R)} = i\left(\mathbf{\Sigma}_{L(R)} - \mathbf{\Sigma}_{L(R)}^\dagger\right). \tag{17}$$

If one uses a complex absorbing potential instead of the self-energy, one simply replaces the self-energy matrices $\mathbf{\Sigma}_L(E)$ and $\mathbf{\Sigma}_R(E)$ with complex potential matrices $\mathbf{W}_L$ and $\mathbf{W}_R$ when defining the spectral densities ($\mathbf{\Lambda}_L$ and $\mathbf{\Lambda}_R$) and the Green's function ($\mathbf{G}$).

We proceed with the analysis of the transmission spectrum for our model. To this end, a useful measure of the deviations of the transmission T_W using our approximations to W from the exact result T_Σ is provided via

$$\Delta T_{max} \equiv \max_{\eta} |T_W(\eta) - T_\Sigma(\eta)| \tag{18}$$

and

$$\Delta T_{ave} \equiv \frac{1}{2} \int_{-1}^{1} d\eta \; |T_W(\eta) - T_\Sigma(\eta)|; \tag{19}$$

η is a dimensionless parameter defined in (14).

1. Tests of Different Approximations to the Complex Potential

We have several possibilities to consider. The first thing we should point out is that, while with the usual local complex potentials it is trivial to define the potential in each electrode, this is not quite as obvious with our potentials. That is, if we follow our procedure as outlined in Sec. II, building the total complex potential

W directly from $\mathbf{H}_0 + \mathbf{\Sigma}_\mathrm{L} + \mathbf{\Sigma}_\mathrm{R}$, we find that it is not, in general, local, and we cannot uniquely define $\mathbf{W}_\mathrm{L}$ and $\mathbf{W}_\mathrm{R}$. For the moment, if we use our procedure to build $\mathbf{H}_0 + \mathbf{W}$ in one step, we write

$$\mathbf{W}_\mathrm{L} = \begin{pmatrix} \mathbf{W}_{LL} & \mathbf{W}_{LM} & \frac{1}{2}\mathbf{W}_{LR} \\ \mathbf{W}_{ML} & \frac{1}{2}\mathbf{W}_{MM} & \mathbf{0} \\ \frac{1}{2}\mathbf{W}_{RL} & \mathbf{0} & \mathbf{0} \end{pmatrix}, \quad (20\mathrm{a})$$

$$\mathbf{W}_\mathrm{R} = \begin{pmatrix} \mathbf{0} & \mathbf{0} & \frac{1}{2}\mathbf{W}_{LR} \\ \mathbf{0} & \frac{1}{2}\mathbf{W}_{MM} & \mathbf{W}_{MR} \\ \frac{1}{2}\mathbf{W}_{RL} & \mathbf{W}_{RM} & \mathbf{W}_{RR} \end{pmatrix}. \quad (20\mathrm{b})$$

On the other hand, we could simply use $\mathbf{H}_0 + \mathbf{\Sigma}_{\mathrm{L(R)}}$ to build $\mathbf{H}_0 + \mathbf{W}_{\mathrm{L(R)}}$, in which case we have a clear and unambiguous way of building the potential due to each electrode at the cost of doing twice as much work. We wish to consider all four possibilities for building **W** given $\mathbf{\Sigma}(E)$ as listed in (10), and for each we wish to see whether it suffices to build **W** directly and from it obtain $\mathbf{W}_\mathrm{L}$ and $\mathbf{W}_\mathrm{R}$ via (20) or if we must build $\mathbf{W}_\mathrm{L}$ and $\mathbf{W}_\mathrm{R}$ separately from the beginning.

In Fig. 1, we show results from each of our four approximations (see Eq. 10), wherein we generate **W** directly; Fig. 2 is identical except that we build $W_{\mathrm{L(R)}}$ separately through $\mathbf{\Sigma}_{\mathrm{L(R)}}$. In all cases, we use $N_\mathrm{L} = N_\mathrm{R} = 100$ and $N = 12$, and compare to the exact result generated by using the self-energy.

Let us first examine the results obtained by constructing **W** directly and extracting $\mathbf{W}_\mathrm{L}$ and $\mathbf{W}_\mathrm{R}$ according to (20). Although none of these results are perfect, we note that most of them are fairly reasonable. Using the unperturbed eigenvectors to build **W** is clearly inadequate to describe the transmission, but already at this crudest level of approximation, we see that we can obtain some qualitative features. Unsurprisingly, simply using the correct eigenvalues is sufficient to put the resonance peaks in the right positions and produce a fair amount of broadening. The unperturbed eigenvectors cannot, however, account for a quantitative description at energies far from the resonance peaks, as they yield overestimated broadenings.

In order to do a reasonable job over the whole energy range, we apparently need to use the correct states. Using the exact states to build $\bar{\mathbf{W}}^\psi$ and $\bar{\mathbf{W}}^\phi$ gives us a transmission function that, except for some relatively small oscillations which are most apparent near the minima, is really quite good. $\bar{\mathbf{W}}^\psi$ and $\bar{\mathbf{W}}^\phi$ yield identical results, as anticipated, and excluding some effects at the band edges that we discuss separately, our deviation measures read $\Delta T_{max} = 0.058$ and $\Delta T_{ave} = 0.014$. Averaging the two, to yield a symmetric complex potential performs almost as well with $\Delta T_{max} = 0.071$ and $\Delta T_{ave} = 0.025$. But $\mathbf{H}_0 + \bar{\mathbf{W}}$ has neither the correct eigenvalues nor the correct eigenstates, again pointing to the importance of using the right states.

Though we can already get reasonable transmission functions by building **W** directly so long as we use the proper states and energy levels, there are still noticeable

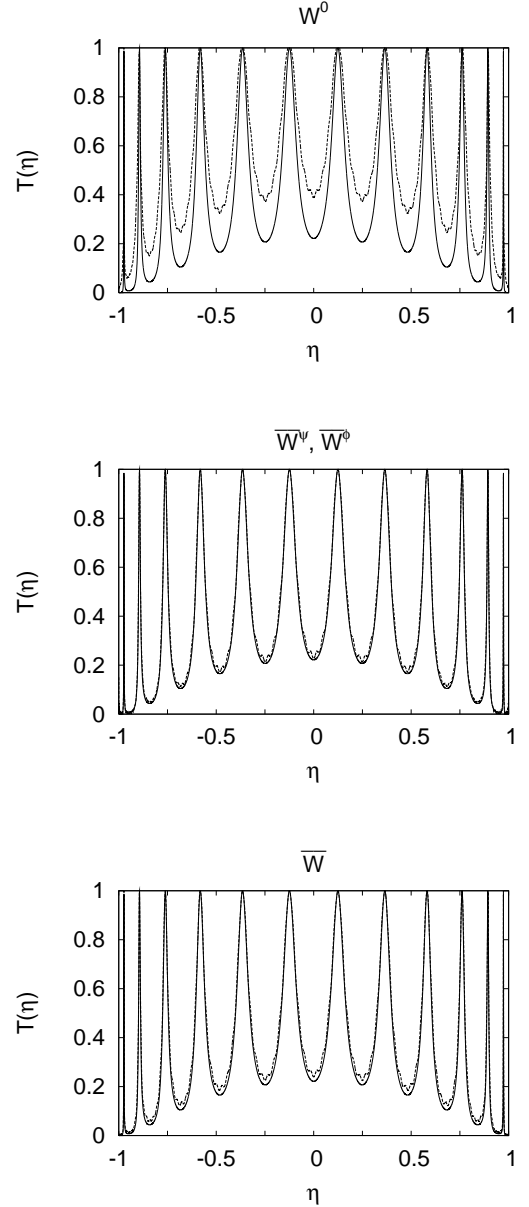FIG. 1: Transmission functions with $N_\mathrm{L} = N_\mathrm{R} = 100$ and $N = 12$ from various approximations used to build **W** directly. The exact result is shown with the heavy line, while the result from our complex potential is given in the dashed line. We recall that $\eta = (E - \epsilon_0)/2\gamma$.

errors which we would like to eliminate. More important, however, is that we have no *a priori* way of defining the potential due to each electrode separately, and our use of (20) to separate $\mathbf{W}_\mathrm{L}$ from $\mathbf{W}_\mathrm{R}$ is largely arbitrary. We can solve both of these problems by building $\mathbf{W}_\mathrm{L}$ and $\mathbf{W}_\mathrm{R}$ separately and combining them to build **W** at the end.

Note first that we must exercise some care if we follow this course. If we were to simply use the eigenvectors **X** of the unperturbed Hamiltonian to do this, we would
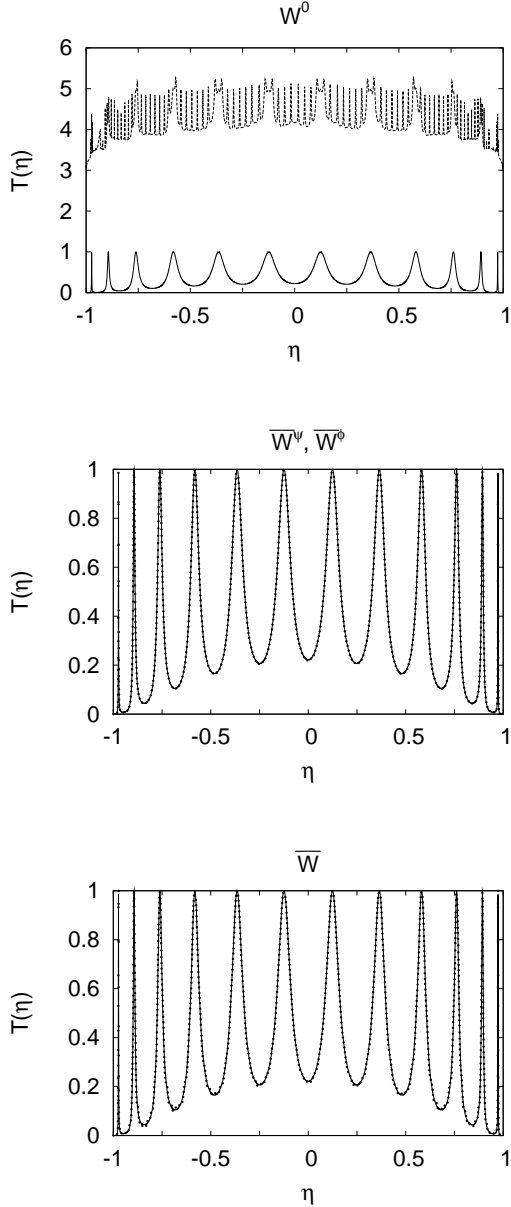
FIG. 2: Transmission functions with $N_L = N_R = 100$ and $N = 12$ from various approximations used to build $\mathbf{W}_L$ and $\mathbf{W}_R$ separately. The exact result is shown with the heavy line, while the result from our complex potential is given in the dashed line (for W^0) or in dots (for $\bar{W}^\psi$, $\bar{W}^\phi$, and $\bar{W}$). We recall that $\eta = (E - \epsilon_0)/2\gamma$.

obtain $\mathbf{W}_L = \mathbf{W}_R = 1/2\,\mathbf{W}$, which is clearly nonsensical and is why the transmission function built from $\mathbf{W}^0$ is meaningless. To amplify on this point, note that under this construction, the spectral densities $\boldsymbol{\Lambda}_L$ and $\boldsymbol{\Lambda}_R$ are diagonal in the same basis as is the Green's function. If the eigenvalues of $\mathbf{H}_0 + \mathbf{W}_L$ and $\mathbf{H}_0 + \mathbf{W}_R$ are $\omega_i =$

$\epsilon_i + 1/2\,\delta_i - 1/2\,\mathrm{i}\,\lambda_i$, then in the diagonal basis we have[37]

$$(\boldsymbol{\Lambda}_L)_{i,i} = \lambda_i \tag{21a}$$

$$(\boldsymbol{\Lambda}_R)_{i,i} = \lambda_i, \tag{21b}$$

$$(\mathbf{G})_{i,i} = \frac{1}{E - \epsilon_i - \delta_i - \mathrm{i}\lambda_i}, \tag{21c}$$

$$(\mathbf{G}^\dagger)_{i,i} = \frac{1}{E - \epsilon_i - \delta_i + \mathrm{i}\lambda_i}. \tag{21d}$$

The transmission function is thus

$$T(E) = \sum_i \frac{\lambda_i^2}{(E - \epsilon_i - \delta_i)^2 + \lambda_i^2}. \tag{22}$$

In other words, it is the sum of N_T independent Lorentzian resonances; this explains the jagged nature of the calculated transmission function, as well as the fact that $T(E)$ is far too large. This should be contrasted with the exact result and with our results using other constructions of $\mathbf{W}$, in which interference between states suppresses all but N peaks in the transmission function.

When, however, we use $\bar{\mathbf{W}}^\psi$ or $\bar{\mathbf{W}}^\phi$, the results are for all practical purposes perfect; $\Delta T_{max} = 0.006$ and $\Delta T_{ave} = 0.001$. While we see a slight degradation in quality from using $\bar{\mathbf{W}}$ instead (with $\Delta T_{max} = 0.093$ and $\Delta T_{ave} = 0.009$), any of these three approaches would be reasonable to take. Once again, the importance of generating the right states is clear.

In the remainder of this work, we will use only $\bar{\mathbf{W}}^\psi$, built by constructing $\mathbf{W}_L$ and $\mathbf{W}_R$ separately, as the results clearly indicate that this is the best way to construct a complex potential among all those that we have considered as demonstrated in the middle panel of Fig. 2[38].

2. Effects of Electrode Size

One of the most interesting features of our complex potential is that the results for the transmission function show an unexpected insensitivity to N_L and N_R. In Fig. 3, we show results for $N = 12$ and for varying electrode sizes N_L and N_R. The results are virtually indistinguishable; we can even choose to use $N_L = N_R = 0$ and still obtain a remarkably accurate transmission function. Of course, the exact transmission function is strictly independent of these parameters, but this observation points to the redundancy of an absorption grid outside the area of interest in similar applications. With a complex potential of the more usual form, this is not necessarily the case. In common implementations, a finite absorption region, whose extent depends on the precise form of the CAP, is essential for the damping of the resonant wave function.

To some extent, this success is illusory. Even our optimal complex potentials do not work as well far from resonance or close to the band edges as they do near a resonance; any residual deviations from the exact results occur at these energies. While the small errors observed
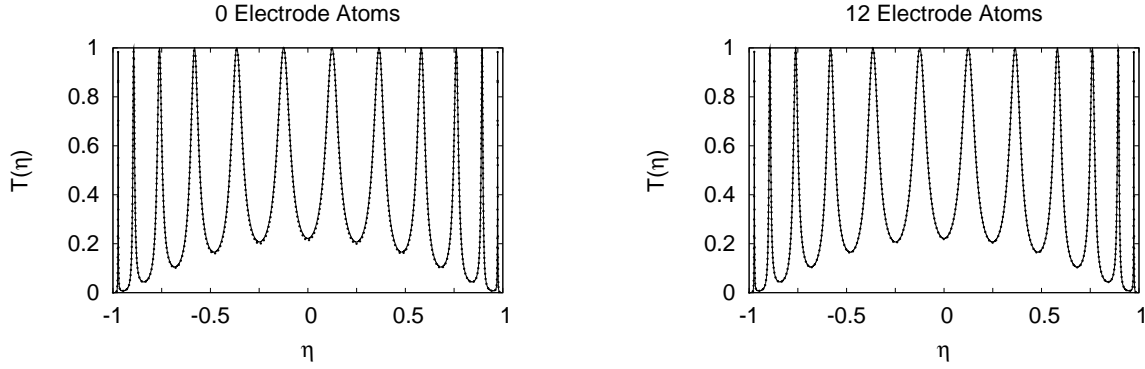
FIG. 3: Transmission as a function of $\eta = (E - \epsilon_0)/2\gamma$ for $N = 12$ with varying N_L and N_R. The exact result is given by the solid line; our results are the dots.

may not be of practical relevance, the electrode extent still plays the major role if stringent convergence is required. We demonstrate this with the following examples.

Resonance Minima - A careful perusal of Fig. 3 reveals that our results are not quite as good near the minima of the transmission function as they are in the resonance peaks. This effect can be seen more readily by decreasing N, which decreases the number of resonances and increases the range of energies far from any of the resonances. In Fig. 4, we show results for $N = 3$ and varying N_L and N_R. We can now see that while once again we can use $N_L = N_R = 0$ to describe the transmission function at resonance, we must use rather large leads if we are to obtain accurate results far from any of the peaks. Indeed, even with $N_L = N_R = 60$, there are still some residual oscillations about the exact result. On the other hand, the deviation measures (18) and (19) decrease monotonically from $\Delta T_{max} = 0.037$ and $\Delta T_{ave} = 0.019$ to $\Delta T_{max} = 0.016$ and $\Delta T_{ave} = 0.004$ as the electrode size varies from $N_L = N_R = 0$ to $N_L = N_R = 60$.

Band Edges - One way to see the difficulty in describing the transmission function near the band edge is to consider the eigenvalues of the matrix $\mathbf{T}(E)$ given by

$$\mathbf{T}(E) = \mathbf{\Lambda}_L \mathbf{G} \mathbf{\Lambda}_R \mathbf{G}^\dagger, \qquad (23)$$

whose trace yields the transmission function. The exact matrix derived from the self-energy has exactly one non-zero eigenvalue at each energy; this eigenvalue is of course numerically equal to the transmission function at that energy. This is to be compared with the results from our calculations using $\bar{\mathbf{W}}^\psi$, displayed in Fig. 5. Near the band edges, we have two non-zero eigenvalues at each energy, and their sum gives us the calculated transmission function. As the energy moves away from the band edge, the smaller of the two eigenvalues goes to zero and we approach the exact result. The precise energy range that marks convergence within a given tolerance depends on the size of the included electrodes. This is readily seen by the eigenvalue plots in Fig. 5 as N_L and N_R increase.

Ideal Wire - A stricter test of our complex potential can be done by calculating the transmission function when the electrode-molecule coupling parameter Γ is set equal to the other coupling parameter, γ. In this case, the exact result is that $T(E) = 1$, as it should be for an ideal wire with no potential sources for scattering. We expect that our complex potential would find this case more difficult to describe, and that the sensitivity to N_L and N_R (or, as we cannot distinguish molecule sites from electrode sites, the sensitivity to N_T) should be much larger than in our previously considered cases. We show results for $N_T = 72$ and for $N_T = 212$ in Fig. 6. Note the reduced range of the ordinate in these plots. In either case, we see small oscillations around the exact result, and we note that the results are considerably worse near the band edge than they are near the middle of the band. The results improve by increasing N_T, again pointing to the role of the electrode size. We believe that the problems near the band edge might be related to the van Hove divergence in the electrode density of states at $E = \pm 2\gamma$. It is worth noting that these same difficulties in describing transmission through an ideal wire are found when phenomenological complex potentials are used in the calculation[39].

3. Structure of the Complex Potential: Non-locality

Now that we have seen how well our complex potential works, it is worthwhile investigating its structure. We will continue to focus on $\bar{\mathbf{W}}^\psi$, and on $\mathbf{W}_L$ and $\mathbf{W}_R$ built separately.

With the bare Hamiltonian and the self-energy that we are using, $\mathbf{W}_L$ and $\mathbf{W}_R$ take a particularly simple structure. For $\mathbf{W}_L$, only the first row is non-zero, and for $\mathbf{W}_R$ only the last row is non-zero; for symmetry reasons it is of course the case that $\mathbf{W}_R$ can be obtained from $\mathbf{W}_L$ by left-right reflection (that is, reflection about the skew diagonal). Elements of the first row of $\mathbf{W}_L$ for $N_L = N_R = 30$ and $N = 12$ are shown in Fig 7. Note that they show a repeating pattern in which each imagi-
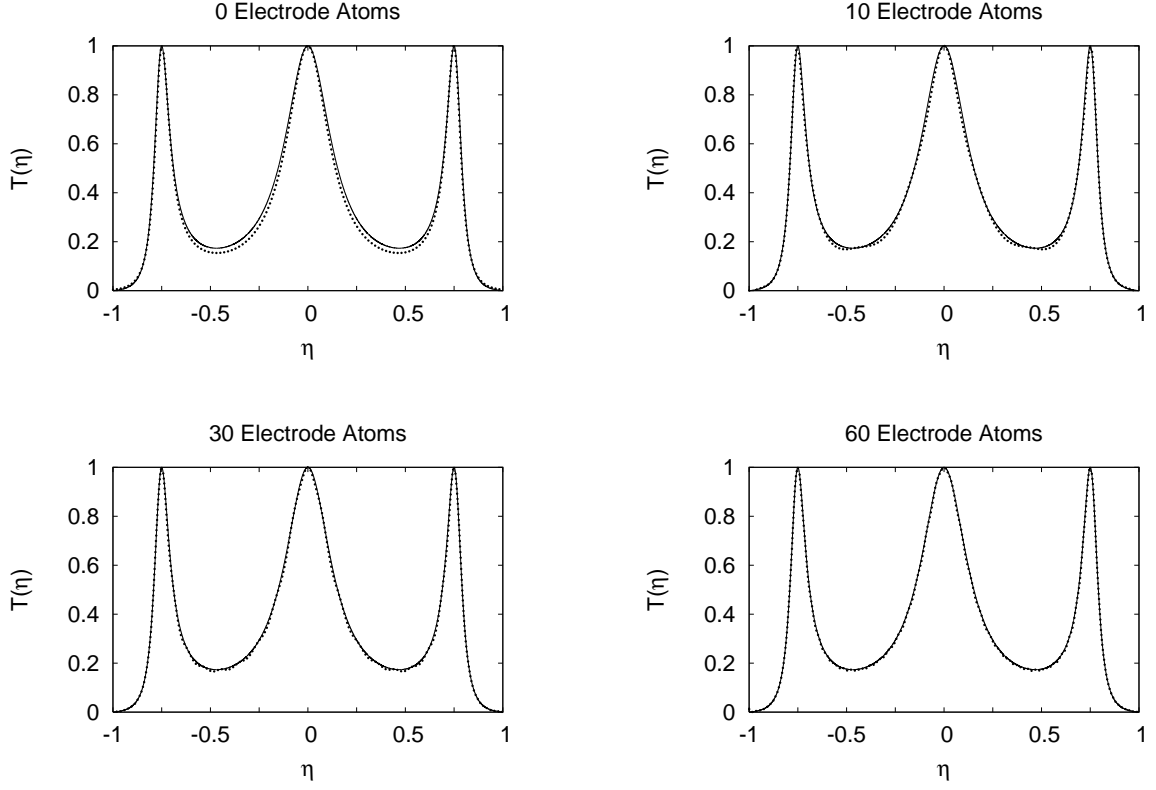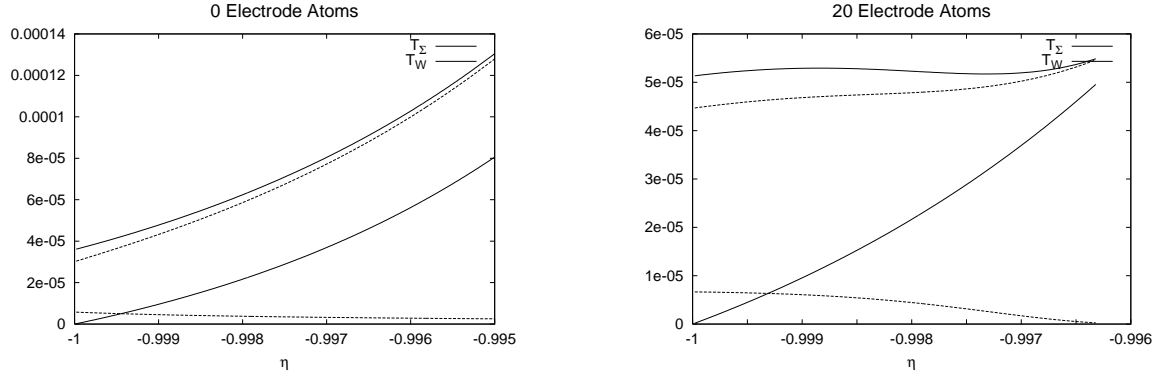
FIG. 4: Transmission as a function of $\eta = (E - \epsilon_0)/2\gamma$ for $N = 3$ with varying N_L and N_R. The exact result is given by the solid line; our results are the dots.

FIG. 5: Transmission function and non-zero eigenvalues of $\mathbf{T}(\eta)$ for $N = 12$ and varying N_L and N_R. The exact transmission function (T_Σ) is displayed in the heavy line; the transmission function calculated using the complex potential (T_W) is displayed in the light line, and the two non-zero eigenvalues of $\mathbf{T}(\eta)$ are given by the dotted line. We recall that $\eta = (E - \epsilon_0)/2\gamma$.

nary element is followed by a real element, and each real element is followed by an imaginary element. Further, while the magnitude of the element typically decreases as one moves from left to right, this is not always the case and there are some relatively significant elements coupling one end of the left electrode to the other end of the right electrode. Our complex potential, in other words, is strongly non-local.

The structure of our complex potential is in sharp distinction to the more common complex potentials. For example, the potential used by Kopf and Saalfrank[35] has the usual structure, namely, the only non-zero elements are negative imaginary and on the diagonal. They vanish within the molecule and the opposite electrode, and increase in magnitude as one moves away from the molecular region.

We have seen that our best complex potentials are non-local, but that the elements far from the diagonal are rather small. This naturally raises the question of just how important the non-locality is. We can study this
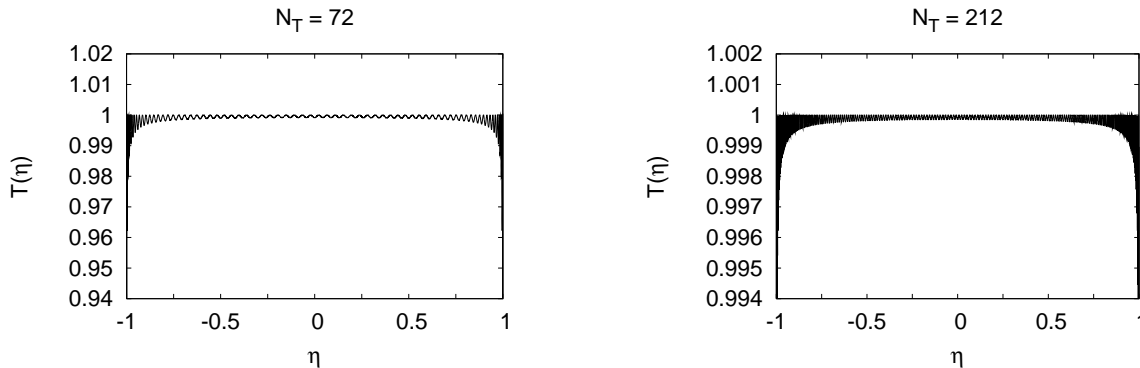
FIG. 6: Transmission as a function of $\eta = (E - \epsilon_0)/2\gamma$ with $\Gamma = \gamma$ for two different values of N_T. The exact result is that $T(\eta) = 1$. Notice the range of the ordinate.
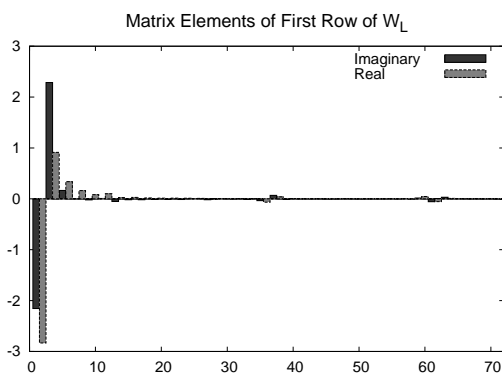

FIG. 7: Elements of the first row of $\mathbf{W}_\mathrm{L}$ for $N_\mathrm{L} = N_\mathrm{R} = 30$ and $N = 12$. Some elements are real; the others are imaginary. None have both real and imaginary parts.

issue by simply constructing the full, non-local complex potential, but, once it is built, removing all but the diagonal (*i.e.*, the fully local part) and some number N_S of the subdiagonals. As N_S approaches $N_\mathrm{T} - 1$, then, we approach the fully non-local CAP in a smooth way. In Fig. 8, we display results for the transmission function with $N_\mathrm{L} = N_\mathrm{R} = 30$, $N = 12$, and several values of N_S.

Clearly, the local approximation is wholly inadequate, and while including only a few subdiagonals improves the results dramatically, there are still deviations from the exact result even with $N_S = 30$. Since there are no such deviations for the fully non-local complex potential, it is clear that the strong non-locality plays a critical role in mimicking the effects of the self-energy.

IV. DISCUSSION AND CONCLUSIONS

We have given a prescription for calculating a complex absorbing potential from the self-energy, thus enabling one to describe coupling to continuum states in an energy-independent way. In our test system, the non-empirical complex potential gives reasonable results even

at the simplest level of approximation, but by obtaining the potential for each electrode individually and using the proper states to construct the potential, we can build a non-local complex potential that yields for most practical purposes essentially the exact transmission function.

We have several main observations to make from this initial work.

First of all, it is essential that the complex potential yield not only the correct energy levels but also the correct states. This is not surprising, as one function of the complex potential is to force free-particle states to look rather like bound states outside of the area of interest. It is no coincidence, then, that inside the area of interest, the states should be greatly modified from the original bound states to closely resemble the resonant eigenfunctions.

Secondly, in cases such as the one we have examined, where there are multiple self-energies in the problem, we should construct a different complex potential for each self-energy, and combine them to form a total complex potential at the end. While we can get away with a somewhat *ad hoc* construction if we have some physical insight, the results are nevertheless not as good as when we build the complex potential for each self-energy separately.

Third, we can, surprisingly, eliminate most of the absorption grid outside the subsystem region of primary interest. This was shown with the explicit elimination of all electrode atoms in our simple system, and it is apparently another consequence of using the correct resonance structure and states. The main effect of increasing the number of explicit electrode atoms (which presumably decreases the burden on the complex potential) is to improve the description at energies off resonance or near the band edge. The great utility of such a significant reduction in the number of required degrees of freedom is readily appreciated if one considers that the bulk metal electrodes can be removed almost completely from electron transport calculations with CAPs.

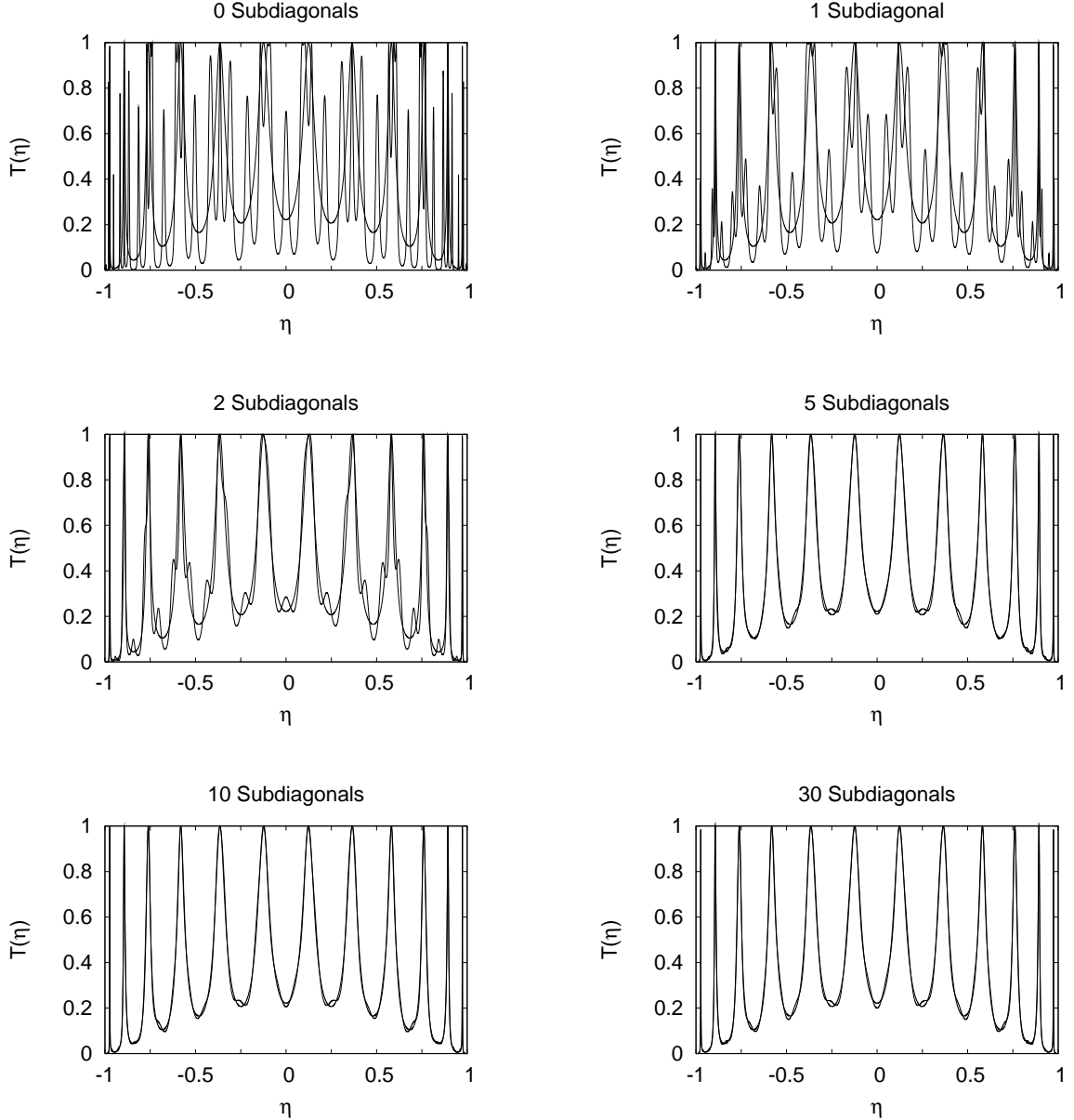Our complex potential works only imperfectly for the ideal wire. Again, most of the problems are at the band

FIG. 8: Transmission function with $N_\mathrm{L} = N_\mathrm{R} = 30$ and $N = 12$ for various values of N_S. The exact result is shown with the heavy line, while the result from our complex potential in a semi-local approximation is given in the lighter line. We recall that $\eta = (E - \epsilon_0)/2\gamma$.

edge, but if we do not include a sufficient number of sites, the description even in the middle of the band has some unphysical oscillations. Of course, in such a system, there are no resonances and one would not really expect a complex potential to describe the physics perfectly anyway. Nevertheless, convergence of the results can be tested as one increases the number of sites explicitly treated.

Finally, our complex potential is strongly non-local, and that non-locality is essential in its functioning. A semi-local approximation is not terrible, and works quite well on resonance, but the full non-locality is needed if we are to accurately describe energies off resonance.

All of this seems to suggest that, so long as one is careful in how one uses a self-energy transformed complex potential of the sort we have introduced, one should easily be able to obtain results within the required accuracy without having to introduce parameters.

A limitation to our approach is the requisite prior knowledge of a self-energy at some level of theory. Therefore, our method is ill-suited to applications for which the self-energy is difficult to construct. However, there is a wide range of problems that can be considered. In the simple case that many-body effects are of major concern only within a subsystem[40] while the surrounding

environment can be adequately treated at the single-particle level, our self-energy transformed complex potential should be easy to construct and would allow us to readily describe the embedded subsystem at a high level of theory. In particular, for quantum transport across molecular junctions it has been shown that many-particle effects[2] can play a critical role, but including the continuum of the reservoirs has proven challenging. Our potentials should enable us to treat the extended molecule with an accurate wave function approach while still including a reasonable description of the bulk electrodes.

[1] G. Cuniberti, G. Fagas, and K. Richter, eds., *Introducing Molecular Electronics*, vol. 680 (Springer, Berlin, 2005).

[2] P. Delaney and J. C. Greer, Phys. Rev. Lett. **93**, 036805 (2004).

[3] G. Fagas, P. Delaney, and J. C. Greer, Phys. Rev. B **73**, 241314 (2006).

[4] M. Koentopp, K. Burke, and F. Evers, Phys. Rev. B **73**, 121403 (2006).

[5] M. Albrecht, B. Song, and A. Schnurpfeil, J. Appl. Phys. **100**, 013702 (2006).

[6] K. S. Thygesen and A. Rubio, cond-mat/0609223.

[7] R. Santra and L. S. Cederbaum, Phys. Rep. **368**, 1 (2002).

[8] J. G. Muga, J. P. Palao, B. Navarro, and I. L. Egusquiza, Phys. Rep. **395**, 357 (2004).

[9] N. Moiseyev, Phys. Rep. **302**, 212 (1998).

[10] W. Domcke, Phys. Rep. **208**, 97 (1991).

[11] H. Feshbach, Ann. Phys. (N.Y.) **5**, 357 (1958).

[12] H. Feshbach, Ann. Phys. (N.Y.) **19**, 287 (1962).

[13] U. Fano, Phys. Rev. **124**, 1866 (1961).

[14] J. S. Bell and E. J. Squires, Phys. Rev. Lett. **3**, 96 (1959).

[15] L. Fonda and R. G. Newton, Ann. Phys. (N.Y.) **10**, 490 (1960).

[16] L. S. Cederbaum, Phys. Rev. Lett. **85**, 3072 (2000).

[17] R. Santra and L. S. Cederbaum, J. Chem. Phys. **117**, 5511 (2002).

[18] S. Feuerbacher, T. Sommerfeld, R. Santra, and L. S. Cederbaum, J. Chem. Phys. **118**, 6188 (2003).

[19] G. Cuniberti, G. Fagas, and K. Richter, Chem. Phys. **281**, 465 (2002).

[20] V. Mujica and M. A. Ratner, Chem. Phys. **326**, 197 (2006).

[21] T. Seideman and W. H. Miller, J. Chem. Phys. **96**, 4412 (1992).

[22] D. Neuhauser, J. Chem. Phys. **103**, 8513 (1995).

[23] J. G. Muga and B. Navarro, Chem. Phys. Lett. **390**, 454 (2004).

[24] D. Macias, S. Brouard, and J. G. Muga, Chem. Phys. Lett. **228**, 672 (1994).

[25] U. V. Riss and H.-D. Meyer, J. Phys. B **28**, 1475 (1995).

[26] A. Vibók and G. G. Balint-Kurti, J. Chem. Phys. **96**, 7615 (1992).

[27] D. E. Manolopoulos, J. Chem. Phys. **117**, 9552 (2002).

[28] B. Poirier and J. T. Carrington, J. Chem. Phys. **118**, 17 (2003).

[29] U. V. Riss and H.-D. Meyer, J. Phys. B **26**, 4503 (1993).

[30] U. V. Riss and H.-D. Meyer, J. Phys. B **31**, 2279 (1998).

[31] N. Moiseyev, J. Phys. B **31**, 1431 (1998).

[32] R. Santra, L. S. Cederbaum, and H. D. Meyer, Chem. Phys. Lett. **303**, 413 (1999).

[33] Y. Sajeev, M. Sindelka, and N. Moiseyev, Chem. Phys. (2006).

[34] G. Fagas, G. Cuniberti, and K. Richter, Phys. Rev. B **63**, 045416 (2001).

[35] A. Kopf and P. Saalfrank, Chem. Phys. Lett. **386**, 17 (2004).

[36] If $|\Psi\rangle$ is an eigenvector of a Hermitian operator, then its Hermitian adjoint $|\Psi\rangle^{\dagger}$ will be the same as its dual $\langle\Psi|$. Because $H_0 + \Sigma$ is non-Hermitian, the dual of one of its eigenvectors will not be the same as its adjoint. In an abuse of notation, we write $\langle\Psi| = |\Psi\rangle^{\dagger}$ even if $|\Psi\rangle$ comes from a non-Hermitian operator. That is, the bra is always meant to indicate the Hermitian adjoint of the ket, rather than its dual.

[37] That there are no factors of one half in the Green's function is because each of $\mathbf{W}_L$ and $\mathbf{W}_R$ contributes $1/2\,\delta_i - 1/2\,i\,\lambda_i$.

[38] We could of course use $\bar{\mathbf{W}}^{\phi}$ instead, as it is equally good.

[39] A. Kopf, private communication.

[40] T. M. Henderson, J. Chem. Phys. **125**, 014105 (2006).